Applied Physics Letters

Cryogenic behavior of NbO_2 based threshold switching devices as oscillation neurons

Cite as: Appl. Phys. Lett. **116**, 162108 (2020); https://doi.org/10.1063/5.0006467
Submitted: 04 March 2020 . Accepted: 09 April 2020 . Published Online: 24 April 2020

Panni Wang, Asif I. Khan, and Shimeng Yu

Cryogenic behavior of NbO_2 based threshold switching devices as oscillation neurons

Cite as: Appl. Phys. Lett. **116**, 162108 (2020); doi: 10.1063/5.0006467
Submitted: 4 March 2020 · Accepted: 9 April 2020 ·
Published Online: 24 April 2020

View Online Export Citation CrossMark

Panni Wang, Asif I. Khan, and Shimeng Yu[a)]

AFFILIATIONS

School of Electrical and Computer Engineering, Georgia Institute of Technology, Atlanta, Georgia 30332, USA

[a)]Author to whom correspondence should be addressed: shimeng.yu@ece.gatech.edu

ABSTRACT

This Letter investigates the cryogenic behavior of NbO_2 threshold switching devices. Pt/NbO_2/Pt devices are demonstrated to be well functional as threshold switching devices at ultra-low temperature (4 K). When the temperature decreases, the OFF-state resistance of NbO_2 increases and the switching voltage increases. With the extracted characteristics of NbO_2 ranging from 4 K to 300 K, we continue to study the neuromorphic system using the crossbar array with resistive memories as resistive synapses and NbO_2 as oscillation neurons at different temperatures through SPICE simulation. The simulation results show that the oscillation systems could still work properly at 4 K. The oscillation amplitude decreases as temperature increases. The oscillation frequency depends on both the temperature and the input voltage.

Deep neural networks (DNNs) have achieved great success in various intelligent tasks such as image classification, speech recognition, and object detection. However, DNNs heavily rely on a large amount of training data and complex networks with hundreds of millions of connections. The data communications between memory and the processor for traditional von Neumann based hardware limit the computing efficiency for DNNs. Therefore, compute-in-memory (CIM), where the computation is directly performed within memory, is proposed to accelerate computation. In this regard, the crossbar array with resistive memories (RRAM) has been proposed to implement the vector-matrix multiplication (VMM),[1–7] the most dominating operation in DNNs. When the input vector (voltage) is fed into the crossbar array, the weighted sum current will sink to the neuro node at the end of the column. Typically, the column current needs to be digitized through integrated-and-fire neurons or analog-to-digital converters (ADCs).[8] However, such circuits are complex and occupy a much larger silicon footprint than the column pitch of the crossbar array, and therefore, the neuron circuit needs to be shared among multi-columns, thereby reducing the computation parallelism.

Recently, NbO_2 has attracted much attention due to its Metal-Insulator-Transition characteristic with potential application as the selector or oscillation neuron.[9–12] NbO_2-based compact threshold switch devices could potentially get rid of the complex CMOS neuron circuit, resulting in a reduced area of $\sim$12.5$\times$ based on the previous circuit-level simulation study.[13] Moreover, previous works have experimentally demonstrated an integrated neuromorphic system with RRAM as resistive synapses and NbO_2 as oscillation neurons.[14,15] Previous work has also characterized the cryogenic behavior of HfOx-based RRAM from 4 K to room temperature.[16] From a technology perspective, neuromorphic computing systems operating in all ranges between room temperature and 4 K are of significant interest both in aerospace electronics and in peripheral control for quantum computers. To date, there is no investigation of the cryogenic behavior of NbO_2-based threshold switch devices. Therefore, it is imperative to investigate the cryogenic behavior of NbO_2. In this Letter, we present a cryogenic characterization of Pt/NbO_2/Pt threshold switching devices. Furthermore, we incorporate the measured results with the RRAM cryogenic behavior[16] and evaluate a neuromorphic system using RRAM as resistive synapses and NbO_2 as oscillation neurons at different temperatures with SPICE simulation.

The Pt/NbO_2/Pt devices were fabricated in the cross-point structure with an active area of $10 \times 10\,\mu m^2$. First, Pt/Ti (25 nm/3 nm) was deposited by e-beam evaporation and patterned through lift-off. Then, a blanket NbO_2 thin film (15 nm) was deposited by reactive sputtering with the Nb target in an O_2/Ar gas mixture at the ratio of 1/10 with the chamber pressure at 4 mTorr, the plasma power of 250 W, and the substrate temperature of 100 °C. The Pt (25 nm) top electrode was formed on the top of NbO_2 by e-beam evaporation and lift-off. The bottom electrode pads were exposed by optical lithography and wet etching of the NbO_2 layer.

The device was characterized in the LakeShore CRX-4K cryogenic probe station using a Keysight B1500 semiconductor device

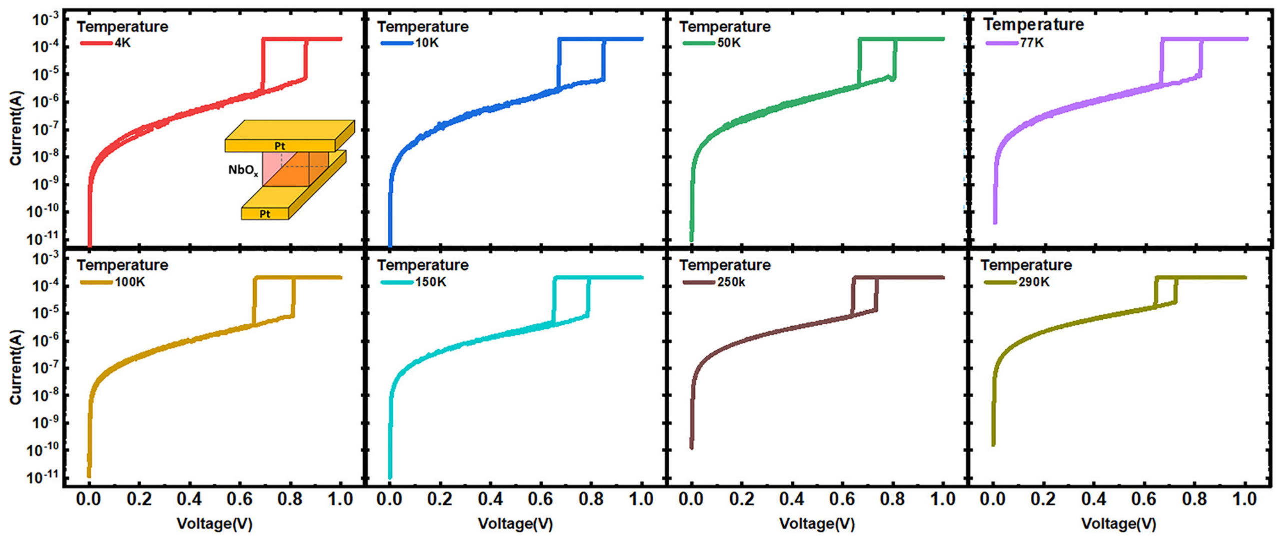

FIG. 1. Measured I–V threshold switching characteristics of the Pt/NbO_2/Pt device at different temperatures down to 4 K. The inset shows the schematic of the fabricated Pt/NbO_2/Pt device.

analyzer. Figure 1 shows the measured threshold switching I–V characteristics of the Pt/NbO_2/Pt devices at different temperatures ranging from 4 K to 290 K. In all the temperature range, as the voltage swept from 0 V to 1 V with a current compliance of 0.2 mA, an abrupt increase in current was observed at the threshold voltage (V_{TH}). While sweeping the voltage back from 1 V to 0 V, the current abruptly decreased to off-current at the hold voltage (V_{HOLD}). This shows that NbO_2 still has exhibited the threshold behavior at 4 K.

To investigate the application of NbO_2 as an oscillation neuron, we further extract its OFF-state resistance (R_{OFF}) and switching voltages. NbO_2 will operate between V_{HOLD} and V_{TH} during the oscillation, and the OFF- Resistance of NbO_2 at 0.7 V is extracted as shown in Fig. 2. R_{OFF} is reduced as the temperature increases from 4 K to 290 K. Previous work[17] showed that the conduction mechanism for Pt/NbO_x/Pt below the threshold voltage is mainly through Frenkel–Poole conduction. When the temperature decreases, the thermal excitation of electrons from traps into the conduction band reduces, thus increasing the resistance. The V_{TH} and V_{HOLD} values at different temperatures are shown in Fig. 3. Both V_{TH} and V_{HOLD} decrease when the temperature increases. The switching voltage almost decreases linearly with the temperature increasing from 4 K to 290 K, which agrees with the NbO_2 switching behavior around the room temperature range (242 K to 380 K) observed in the previous study.[17] Finally, we fit the log(R_{OFF})-T, V_{TH}-T, and V_{HOLD}-T curves with linear regression and sweep the temperature to obtain R_{OFF}, V_{TH}, and V_{HOLD} parameters at different temperatures for SPICE simulation.

Combining the parameters for NbO_2 devices and RRAM resistance[16] ranging from 4 K to 300 K as shown in Table I, we continue to evaluate the neuromorphic systems using RRAM as resistive synapses

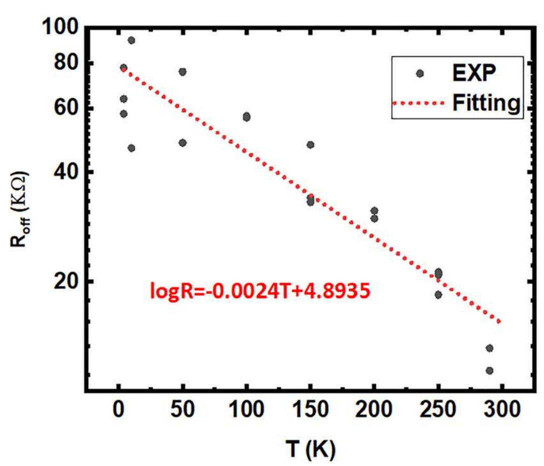

FIG. 2. The temperature dependence of NbO_2 OFF-state resistance. The resistance is read at 0.7 V.

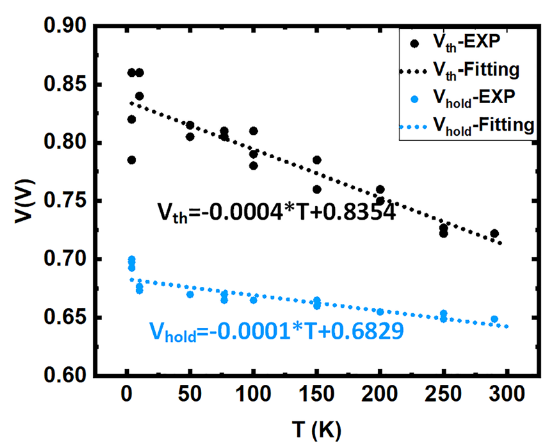

FIG. 3. Temperature dependence of the threshold voltage (V_{th}) and hold voltage (V_{hold}) extracted from the current–voltage characteristic of Fig. 1.

TABLE I. Oscillation simulation parameters.

T(K)	R_{OFF}(KΩ)	V_{TH}(V)	V_{HOLD} (V)	R_{RRAM} (KΩ)[16]
4	76.57	0.8338	0.6823	33.0
10	74.12	0.8313	0.6815	33.0
50	59.64	0.8148	0.6761	31.8
100	45.53	0.7942	0.6694	29.4
150	34.65	0.7735	0.6627	26.6
200	26.41	0.7529	0.6559	23.1
250	20.13	0.7323	0.6492	20.4
300	15.33	0.7117	0.6425	18.1

and NbO_2 as oscillation neurons at different temperatures through SPICE simulation. The circuit configuration is shown in Fig. 4(a). The RRAM and NbO_2 are connected in series, and there is a parasitic capacitor at the neuron node. The parasitic capacitor is set to 100 fF in simulation, representing the column parasitic capacitance from the RRAM array.[13] The input voltage is applied through the top side of RRAM, and the output voltage is read from the neuron node. Initially, NbO_2 is in the OFF state; when the input voltage (V_{DD}) is applied, the parasitic capacitor will be charged. According to the voltage divider rule, the neuron node should be charged up to $V_{DD} \times R_{OFF}/(R_{OFF} + R_{RRAM})$. If the node voltage is larger than the threshold voltage, NbO_2 will be turned on and its resistance will be reduced to R_{ON}. Then, the neuron node voltage will be reduced, resulting in capacitor discharge. The neuron node voltage will be discharged down to $V_{DD} \times R_{ON}/(R_{ON} + R_{RRAM})$. Similarly, if this discharged voltage is less than V_{HOLD}, NbO_2 will be turned off. Thus, the neuron node voltage oscillates between V_{HOLD} and V_{TH}. To achieve the oscillation, the NbO_2 device should be cycled multiple times between the OFF state and the ON state. NbO_2 threshold switching endurance testing showed that its switching characteristics were not degraded up to 10^6 cycles at room temperature,[18] which is sufficient for neuromorphic applications. Furthermore, the following requirements should be satisfied:

$$\frac{V_{DD} \times R_{OFF}}{R_{OFF} + R_{RRAM}} \geqslant V_{TH}, \tag{1}$$

$$\frac{V_{DD} \times R_{ON}}{R_{ON} + R_{RRAM}} \leqslant V_{HOLD}. \tag{2}$$

Since R_{ON} (~1 KΩ) is much smaller than R_{RRAM} (~30 KΩ), then $R_{ON}/(R_{ON} + R_{RRAM}) \gg 1$; therefore, requirement (2) can be easily satisfied. It should be noted that $R_{OFF} < R_{RRAM}$ is not a must. Even if $R_{OFF} > R_{RRAM}$, requirement (1) could still be satisfied with large enough V_{DD}.

During the characterization, since the compliance current is set to avoid destroying the devices, the actual R_{ON} is not obtained. However, during the oscillation, the charging is mainly through OFF-state NbO_2 and discharging is mainly through the RRAM since RRAM resistance is much larger than that of the ON-state NbO_2. Therefore, the oscillation frequency mainly depends on R_{OFF} and R_{RRAM}. During the simulation, the R_{ON} value is set to 1 KΩ, which will not affect the results. It should be noted that the ON/OFF ratio for NbO_2 is typically 100,[19,20] and the extracted highest R_{OFF} is 76 KΩ at 4 K. Therefore, 1 KΩ is a reasonable value for R_{ON}. During the SPICE simulation, NbO_2 is modeled with a Verilog-A behavior model that captures the switching characteristics with parameters such as the resistance in the ON/OFF state (R_{ON}/R_{OFF}), the threshold voltage (V_{TH}), and the hold voltage (V_{HOLD}).[13] The intrinsic transition time between the ON/OFF state is set to 10 ps.[13] Figures 4(b)–4(e) show the simulation results of the output voltage waveform for 4 K and 300 K at different V_{DD} values. When the square pulse is fed into the input, the output neuron waveform oscillates. We sweep the temperature from 4 K to 300 K, the output oscillation frequency and oscillation amplitude are shown in Figs. 5 and 6, respectively. It shows that the oscillation amplitude is between V_{HOLD} and V_{TH} and it decreases when the temperature increases. Therefore, the oscillation amplitude is mainly determined by V_{HOLD} and V_{TH}. The oscillation amplitude modulation depends on NbO_2 device optimization such as NbO_2 film thickness tuning[18] and device structure engineering.[19] The oscillation frequency is related to not only temperature but also V_{DD}. It can be further described analytically by solving the equation[13] based on Kirchhoff's Law on the configuration. The charging time t_{rise} and discharging time t_{all} are expressed by the following equations:

$$t_{rise} = R_{rise} C \times \log \frac{V_{DD}\frac{R_{rise}}{R_{RRAM}} - V_{HOLD}}{V_{DD}\frac{R_{rise}}{R_{RRAM}} - V_{TH}} = R_{rise} C \times \log A_{rise}, \tag{3}$$

$$t_{all} = R_{all} C \times \log \frac{V_{DD}\frac{R_{all}}{R_{RRAM}} - V_{HOLD}}{V_{DD}\frac{R_{all}}{R_{RRAM}} - V_{TH}} = R_{all} C \times \log A_{all}, \tag{4}$$

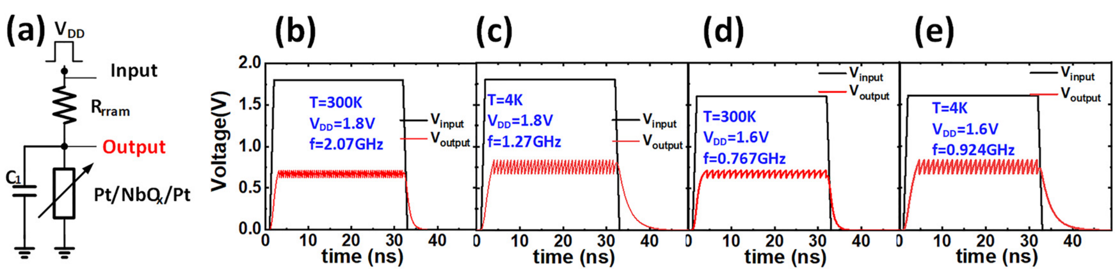

FIG. 4. (a) Circuit configuration of an oscillation neuron node with the Pt/NbO_2/Pt device and a RRAM as synapse. Simulated oscillation waveforms with various V_{DD} and temperature values: (b) V_{DD} = 1.8 V and T = 300 K, (c) V_{DD} = 1.8 V and T = 4 K, (d) V_{DD} = 1.6 V and T = 300 K, and (e) V_{DD} = 1.6 V and T = 4 K.

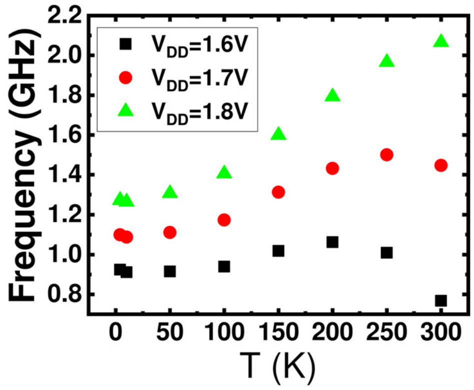

FIG. 5. Temperature dependence of the oscillation frequency with different input V_{DD} values.

where $R_{rise} = R_{RRAM} \parallel R_{OFF}$ and $R_{all} = R_{RRAM} \parallel R_{ON}$. The rise time and fall time depend on both the RC product and the parameter A_{rise}/A_{all}. The RC product decreases when the temperature increases as R_{OFF} of NbO_2 and R_{RRAM} decreases. However, the parameters A_{rise}/A_{all} will increase with the temperature. When V_{DD} is large, A_{rise} or A_{all} is close to 1, and the RC product will dominate the oscillation time. When V_{DD} is small (e.g., $V_{DD} = 1.6$V), $A_{rise} = 1.53$ at T = 4 K and $A_{rise} = 4.01$ at T = 300 K. Therefore, the final oscillation time depends on both the RC product and V_{DD}.

In summary, the cryogenic behavior of NbO_2-based threshold switching devices is characterized in this work. First, the device still has the threshold switching behavior at an ultra-low temperature of 4 K, showing promise for cryogenic applications. Second, the resistance and switching voltages at different temperatures are extracted. The NbO_2 resistance decreases and the switching voltages decrease when the temperature increases. Finally, with the extracted parameters, we evaluate the neuromorphic system using RRAM as resistive synapses and NbO_2 as oscillation neurons at different temperatures through SPICE simulation. The neuron oscillation system still works at 4 K with possibly lower oscillation frequency but higher oscillation amplitude. The oscillation amplitude is mainly between V_{HOLD} and V_{TH} depending on the temperature. The oscillation frequency depends on both the input voltage and the temperature.

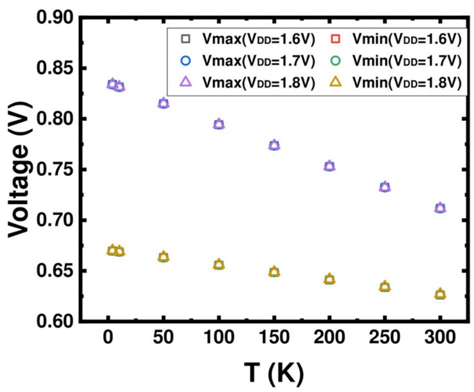

FIG. 6. Temperature dependence of the oscillation amplitude with different input V_{DD} values.

We thank Jiyong Woo for help in device fabrication. This work was in part supported by No. NSF-ECCS-1903577.

The data that support the findings of this study are available from the corresponding author upon reasonable request.

REFERENCES

[1]S. Yu, "Neuro-inspired computing with emerging nonvolatile memorys," Proc. IEEE **106**, 260–285 (2018).
[2]X. Si, J. Chen, Y. Tu, W. Huang, J. Wang, Y. Chiu, W. Wei, S. Wu, X. Sun, R. Liu, S. Yu, R. Liu, C. Hsieh, K. Tang, Q. Li, and M. Chang, "24.5 a twin-8T SRAM computation-in-memory macro for multiple-bit CNN-based machine learning," in IEEE International Solid-State Circuits Conference—(ISSCC) (2019), pp. 396–398.
[3]G. W. Burr, R. M. Shelby, C. di Nolfo, J. W. Jang, R. S. Shenoy, P. Narayanan, K. Virwani, E. U. Giacometti, B. Kurdi, and H. Hwang, "Experimental demonstration and tolerancing of a large-scale neural network (165,000 synapses), using phase-change memory as the synaptic weight element," in IEEE International Electron Devices Meeting (2014), pp. 29.5.1–29.5.4.
[4]W. Kim, R. L. Bruce, T. Masuda, G. W. Fraczak, N. Gong, P. Adusumilli, S. Ambrogio, H. Tsai, J. Bruley, J. Han, M. Longstreet, F. Carta, K. Suu, and M. BrightSky, "Confined PCM-based analog synaptic devices offering low resistance-drift and 1000 programmable states for deep learning," in Symposium on VLSI Technology (2019), pp. T66–T67.
[5]M. Prezioso, F. Merrikh-Bayat, B. Hoskins, G. C. Adam, K. K. Likharev, and D. B. Strukov, "Training and operation of an integrated neuromorphic network based on metal-oxide memristors," Nature **521**, 61–64 (2015).
[6]W. Wu, H. Wu, B. Gao, P. Yao, X. Zhang, X. Peng, S. Yu, and H. Qian, "A methodology to improve linearity of analog RRAM for neuromorphic computing," in *IEEE Symposium on VLSI Technology* (IEEE, 2018), pp. 103–104.
[7]F. Cai, J. M. Correll, S. H. Lee, Y. Lim, V. Bothra, Z. Zhang, M. P. Flynn, and W. D. Lu, "A fully integrated reprogrammable memristor–CMOS system for efficient multiply-accumulate operations," Nat. Electron. **2**, 290–299 (2019).
[8]D. Kadetotad, Z. Xu, A. Mohanty, P.-Y. Chen, B. Lin, J. Ye, S. Vrudhula, S. Yu, Y. Cao, and J.-S. Seo, "Parallel architecture with resistive crosspoint array for dictionary learning acceleration," IEEE J. Emerging Sel. Top. Circuits Syst. **5**, 194–204 (2015).
[9]S. Kumar, Z. Wang, N. Davila, N. Kumari, K. J. Norris, X. Huang, J. P. Strachan, D. Vine, A. D. Kilcoyne, Y. Nishi *et al.*, "Physical origins of current and temperature controlled negative differential resistances in NbO_2," Nat. Commun. **8**, 658 (2017).
[10]K. Moon, E. Cha, J. Park, S. Gi, M. Chu, K. Baek, B. Lee, S. Oh, and H. Hwang, "High density neuromorphic system with $Mo/Pr_{0.7}Ca_{0.3}MnO_3$ synapse and NbO_2 IMT oscillator neuron," in IEEE International Electron Devices Meeting (IEDM) (2015), pp. 17.6.1–17.6.4.
[11]S. Li, X. Liu, S. K. Nandi, D. K. Venkatachalam, and R. G. Elliman, "High-endurance megahertz electrical self-oscillation in Ti/NbO_x bilayer structures," Appl. Phys. Lett. **106**, 212902 (2015).
[12]E. Cha, J. Park, J. Woo, D. Lee, A. Prakash, and H. Hwang, "Comprehensive scaling study of NbO_2 insulator-metal-transition selector for cross point array application," Appl. Phys. Lett. **108**, 153502 (2016).
[13]P.-Y. Chen, J.-S. Seo, Y. Cao, and S. Yu, "Compact oscillation neuron exploiting metal-insulator-transition for neuromorphic computing," in *IEEE/ACM International Conference on Computer-Aided Design (ICCAD)* (IEEE, 2016), pp. 1–6.
[14]L. Gao, P.-Y. Chen, and S. Yu, "NbO_x based oscillation neuron for neuromorphic computing," Appl. Phys.. Lett. **111**, 103503 (2017).
[15]J. Woo, P. Wang, and S. Yu, "Integrated crossbar array with resistive synapses and oscillation neurons," IEEE Electron Device Lett. **40**, 1313–1316 (2019).
[16]R. Fang, W. Chen, L. Gao, W. Yu, and S. Yu, "Low-temperature characteristics of HfO_x-based resistive random access memory," IEEE Electron Device Lett. **36**, 567–569 (2015).

[17]S. Slesazeck, H. Mähne, H. Wylezich, A. Wachowiak, J. Radhakrishnan, A. Ascoli, R. Tetzlaff, and T. Mikolajick, "Physical model of threshold switching in NbO_2 based memristors," RSC Adv. **5**, 102318–102322 (2015).

[18]E. Cha, J. Woo, D. Lee, S. Lee, J. Song, Y. Koo, J. Lee, C. G. Park, M. Y. Yang, K. Kamiya, K. Shiraishi, B. Magyari-Köpe, Y. Nishi, and H. Hwang, "Nanoscale (∼10 nm) 3D vertical ReRAM and NbO_2 threshold selector with TiN electrode," in IEEE International Electron Devices Meeting (2013), pp. 10.5.1–10.5.4.

[19]M. Kang and J. Son, "Off-state current reduction in NbO_2-based selector device by using TiO_2 tunneling barrier as an oxygen scavenger," Appl. Phys. Lett. **109**, 202101 (2016).

[20]X. Liu, S. K. Nandi, D. K. Venkatachalam, K. Belay, S. Song, and R. G. Elliman, "Reduced threshold current in NbO_2 selector by engineering device structure," IEEE Electron Device Lett. **35**, 1055–1057 (2014).